J Wood Sci (1999) 45:10–18

ORIGINAL ARTICLE

Masashi Nakamura · Minoru Masuda · Kanako Shinohara

Multiresolutional image analysis of wood and other materials

Received: April 22, 1998 / Accepted: September 2, 1998

Abstract The gloss of wood is a unique texture compared to that of other materials. To express it quantitatively, two digital-image analyses were performed. One method was multiresolutional contrast analysis, which was the new method developed in this study. The other method was fractal image analysis. Twenty-four specimens, including solid woods, wood-plastic composites (WPCs), printed grains, and granites, were prepared. Digital images of specimens were obtained in five sizes and in two illuminant directions (perpendicular and parallel to the grain). The multiresolutional contrast values of perpendicular illuminated images were calculated and compared among specimens. The result of this quantitative analysis was that the gloss of wood was characterized by bright spots in a relatively small area. Using fractal analysis, the fractal dimension of a digital image was used as an index of brightness changes, not for expressing the self-similarity. These indices showed results similar to those of the multiresolutional contrast analysis.

Key words Multiresolutional contrast · Fractal analysis · Gloss of wood · Texture analysis · Digital image analysis

Introduction

Gloss plays one of the most important roles in the appearance of various materials. Particularly, the gloss of wood is full of variety owing to its anatomical structures and shows optical anisotropy. This appearance of wood is unique compared to other materials, such as metals, glasses, and plastics.

When we observe the gloss of a material, we see it as a two-dimensional image of light reflection and then feel or evaluate various psychological images concerning it. Therefore, if we investigate the influence of gloss on psychological visual images, we must describe gloss quantitatively and two-dimensionally.

In previous studies the gloss of various materials, including woods and wood-based materials, was measured using a goniophotometer.[1–3] Conventional goniophotometry brought important information about light reflection on the surface of materials, but using goniophotometry made it difficult to measure the two-dimensional distribution of gloss because it was a spot measurement.

In this study, to describe and evaluate the gloss of material surfaces quantitatively and two-dimensionally, we carried out two digital-image analyses and examined the validity of the two methods. One method utilized multiresolutional contrast analysis, and the other one was fractal analysis. The former method was based on calculation of multiresolutional contrast of the digital image. The latter method was based on calculation of the fractal dimension of an image. Using both methods, we quantitatively compared the gloss of wood and other materials.

Experiments

Specimens

Twenty-four specimens were prepared in this study: seven solid wood specimens finished with a planer, two clear-varnished wood specimens, two wood–plastic composite specimens (WPC), one particleboard (PB), two milled wood powder–plastic composite specimens (MWPC), six printed-sheet overlaid boards (printed grain), two pieces of paper, and two granites. The details are shown in Table 1.

M. Nakamura (✉) · M. Masuda · K. Shinohara[1]
Division of Forest and Biomaterials Science, Graduate School of Agriculture, Kyoto University, Kyoto 606-8502, Japan
Tel. +81-75-753-6237; Fax +81-75-753-6300
e-mail: nakamasa@h1sparc1.kais.kyoto-u.ac.jp

[1] *Present address*: Central Research Laboratory, Daiwa House Industry Co., Ltd., Sakyo, Nara 631-0801, Japan

* Part of this paper was presented at the 47th annual meeting of the Japan Wood Research Society in Kochi, April 1997

Table 1. Specimens used in this study

Category and nos.	Specimens	Features
Solid wood		
S1	Douglas fir (*Pseudotsuga menziesii*)	Edge grain, planer-finished surface
S2	Hinoki (*Chamaecyparis obtusa*)	Edge grain, planer-finished surface
S3	Sugi (*Cyptomeria japonica*)	Edge grain, planer-finished surface
S4	Mizunara (*Quercus crispula*)	Edge grain, planer-finished surface
S5	Maple (*Acer mono* Maxim)	Edge grain, planer-finished surface
S6	Maple (*Acer* sp.)	Wavy grain, planer-finished surface, fancy veneer-overlaid plywood
S7	Keyaki [*Zelkova serrata*]	Edge grain, planer-finished surface
Varnished		
V1	Keyaki	Edge grain, clear-varnished surface
V2	Keyaki	Flat grain, clear-varnished surface, tray product
WPC[a]		
W1	No. 1 (Douglas fir)	Flat grain, a piece of floor parquet products
W2	No. 2 (Mizunara)	Edge grain, a piece of floor parquet products
MWPC[b]		
M1	No. 1	Oak appearance
M2	No. 2	Cherry appearance
Other wood-based material		
B1	Particleboard	
Printed grain		
P1	No. 1	Oak appearance
P2	No. 2	Oak appearance
P3	No. 3	Oak appearance
P4	No. 4	Oak appearance
P5	No. 5	Oak appearance
P6	No. 6	Oak appearance
Paper		
J1	Japanese paper	White color
J2	Gray paper PANTONE U464	Gray color
Granite		
G1	No. 1	Black and white speckles, polished
G2	No. 2	Black and white speckles, burner-jet finished

[a] Wood–plastic composite.
[b] Milled wood powder–plastic composite

All of the specimens had enough dimensions to obtain digital images.

Gloss images

The image capturing system (Fig. 1) consisted of a charge-coupled device (CCD) monochrome video camera (XC-77; Sony, Tokyo, Japan) with a macro lens (Micro Nikkor 55 mm; Nikon, Tokyo, Japan), a photo copy stand, a turntable, and a high intensity cold lighting system (Cold Spot; Nippon P.I., Tokyo, Japan). Specimens were placed on the turntable and illuminated from an oblique angle (45°). The center of the turntable was adjusted to the optical axis of the video camera. This system was set up in a dark room.

Adjusting the height and the focus of a video camera, images were captured in five sizes: 4 × 4 mm, 8 × 8 mm, 16 × 16 mm, 32 × 32 mm, and 64 × 64 mm. A captured image was digitized to 512 × 512 pixels and 8 bit (256 steps) gray levels by the image analyzer (Luzex III, Nireco, Hachioji, Japan). The digital-image resolutions per pixel were about 8, 16, 31, 63, and 125 μm for each capturing size. The incident direction for a specimen was changed by rotating the turntable. In this study, images were captured with two incident directions: parallel and perpendicular to the grain. For nonwood specimens the two incident directions were parallel and perpendicular to the long side of a specimen. A total of 10 digital images (five captured sizes and two incident directions) were recorded for each specimen. The horizontal direction of each digital image was perpendicular to the grain (or the long side of a nonwood specimen).

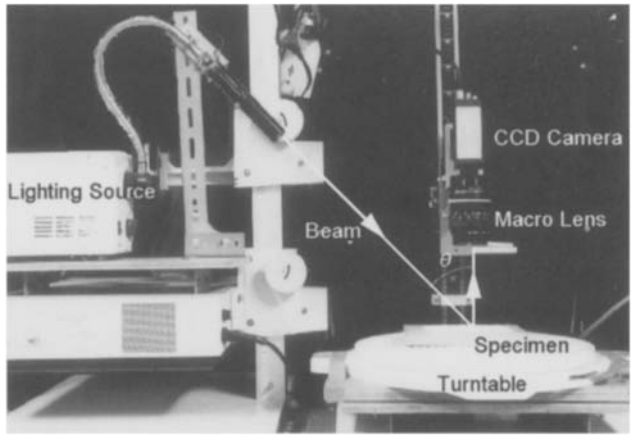

Fig. 1. Arrangement of equipment used for capturing gloss images. Incident angle θ is 45°

We call the digital images "gloss images." The four photographs in the second line of Fig. 2 are gloss images of

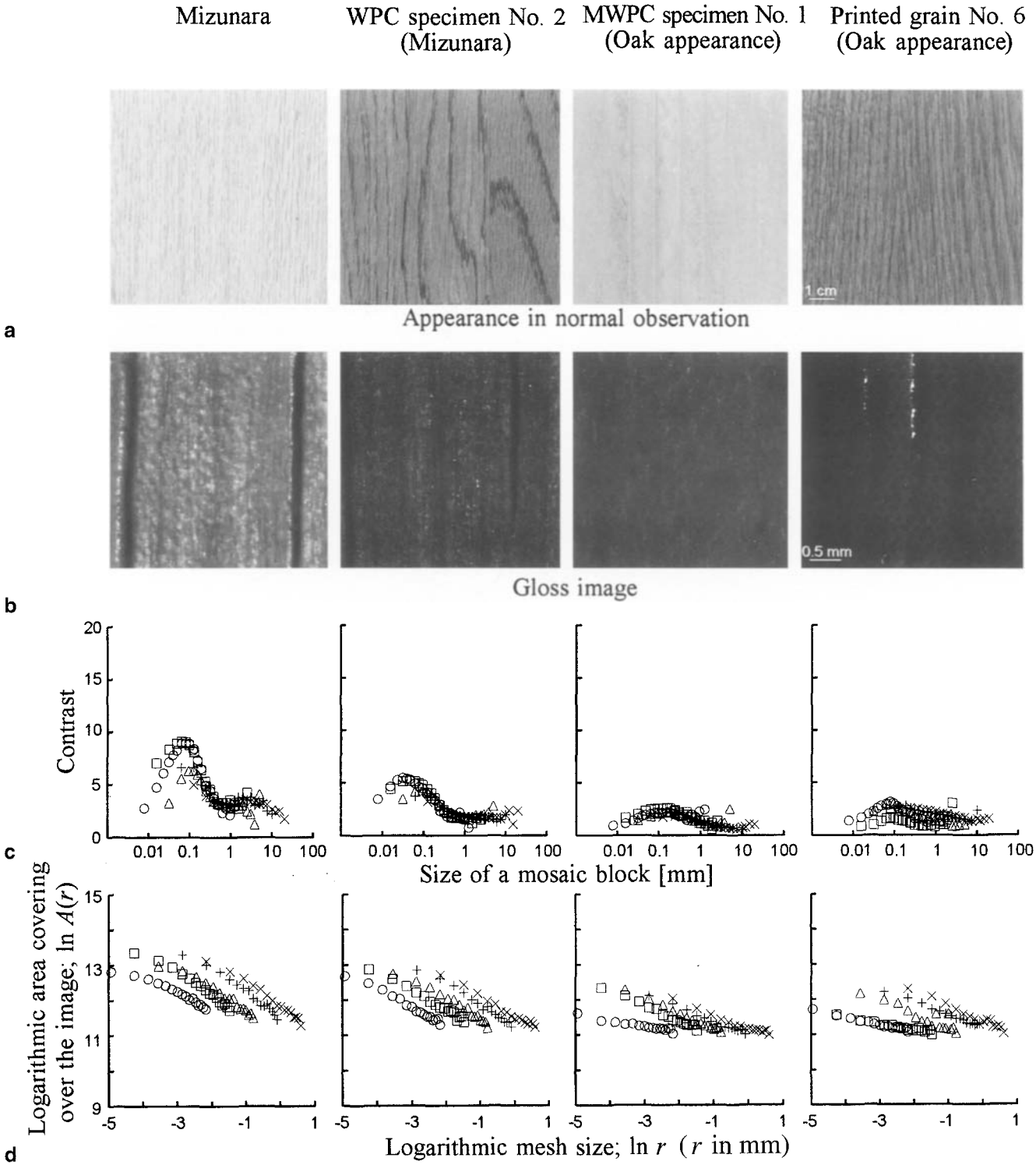

Fig. 2. Examples of appearances of specimens, gloss images, multiresolutional contrast analysis, and fractal analysis. **a** Appearances of specimens in the normal observations. **b** Gloss images (4 mm square type). **c** Distributions of multiresolutional contrasts. **d** Results of the fractal analysis. *Circles*, 4 mm square gloss image; *squares*, 8 mm square gloss image; *triangles*, 16 mm square gloss image; *pluses*, 32 mm square gloss image; *crosses*, 64 mm square gloss image

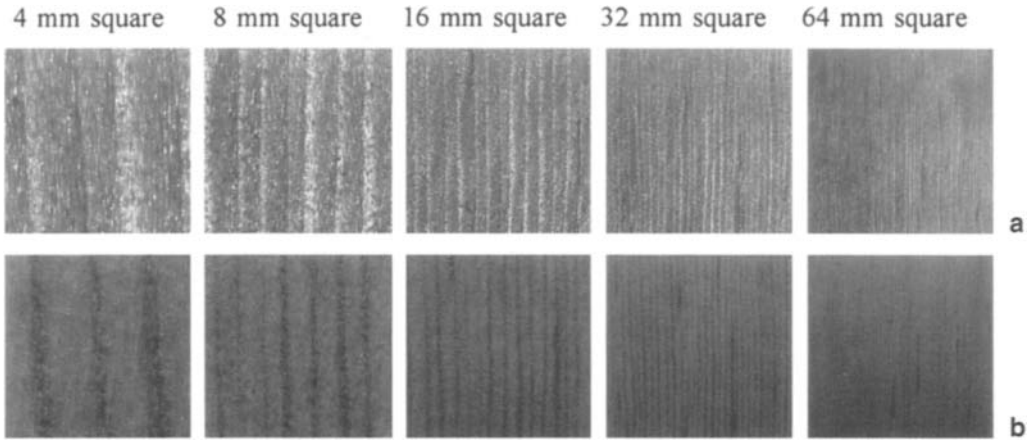

Fig. 3. Example of gloss images in five sizes [Douglas fir (*Pseudotsuga menziesii*)]. **a** Illuminated perpendicular to the grain. **b** Illuminated parallel to the grain

various specimens. The 10 photographs in Fig. 3 are gloss images of Douglas fir.

Adjustment of gloss images

Shading correction

An image of a standard white plate was captured and digitized under the same conditions before measuring the specimens and was subtracted from the gloss image. As a result of this simple shading correction, undesirable subtle shadings were almost eliminated from the original gloss image. Shading-corrected gloss images were used for the calculations.

Gray level conversion to the tristimulus value Y

Gray levels were of relative value depending on the digital imaging devices. It was inconvenient to show the real brightness in the multiresolutional contrast analysis so a converting equation was derived by the following procedure. Thirty-seven images of gray chip (Munsell neutral value scale from full black to full white) were captured, digitized, and corrected in the same manner as the gloss images, and a mean gray level was calculated for each. Then their tristimulus values were measured by a colorimeter (Z-1001DP, Nippon Denshoku Kogyo, Tokyo, Japan). As a result, good linear relations between gray levels and the tristimulus value (*Y*s) were observed, and the converting equation of gray level to *Y* was derived. Using this equation, results of the multiresolutional contrast analysis were converted to the tristimulus value *Y*s.

Multiresolutional contrast analysis

As shown in the second line of Fig. 2 or Fig. 3, bright spots are scattered in gloss images. To analyze those distributions, the spatial frequency analysis based on the two-dimensional fast Fourier transform (2D-FFT) was often used.[4–8] Although 2D-FFT easily displays a power spectrum map as an image, it is difficult to extract a unique value expressing the characteristics of the image.

In former reports,[9,10] authors proposed the pattern numerization method based on local-area contrast in an image. This method was basically a one-dimensional image analysis that used a digital-image filter of a certain size and calculated some statistics concerned with local-area contrast. In our study, multiresolutional contrast analysis was proposed as a new method. Although this method was based on the same concept as the one-dimensional analysis, it was extended two-dimensionally and size-variable filters were used. For a general image analysis, various image filters are used to extract characteristics from an image. Here, because a large image filter extracted large features in an image and a small filter extracted small ones, the use of size-variable filters was necessary to perform the multiresolutional image analysis.

The multiresolutional contrast analysis is performed and expressed by the following procedure and equations. In the first step, a gloss image $F(i, j)$ ($1 \leq i \leq m$, $1 \leq j \leq n$; m, n: horizontal and vertical image sizes, respectively) was transformed to a set of mosaic images (Fig. 4). Making a mosaic image meant image filtering. It is denoted by Eq. (1).

$$G_k(I, J) = \frac{1}{k^2} \sum_{p=1}^{k} \sum_{q=1}^{k} F(i_k + p, j_k + q) \tag{1}$$

where k is the filter size, $G_k(I, J)$: mosaic-image smoothed by size k filter, $F(i_k + p, j_k + q)$: original gloss image. The mosaic (or filter) size k was defined by the following manner:

$$k_h = k_v = k \qquad (1 \leq k_h \leq m,\ 1 \leq k_v \leq n),$$

where k_h is the horizontal filter size; k_v is the vertical filter size; (I, J) is the location of a mosaic in G_k [$1 \leq I \leq M$, $1 \leq J \leq N$; $M = m / k_h$, $N = n / k_v$]; and $(i_k + p, j_k + q)$ is the location of a pixel in F [$i_k = (I - 1)k$, $j_k = (J - 1)k$].

In this study m and n were both set to 480 pixels ($m = n$, and so $M = N$). Although a gloss image was composed of 512 × 512 pixels, as mentioned above, the effective area suitable for the analysis was 480 × 480 pixels. Mosaic size k

had 22 variations from 1 pixel to 160 pixels per block. The minimum size of a mosaic block was an 8-μm square in a 4-mm square gloss image; the maximum size was 20-mm square in a 64-mm square gloss image.

In the next step, differences between adjacent mosaic blocks were calculated.

$$
\begin{aligned}
C_{kh}(I,J) &= \left|\{G_k(I,J) - G_k(I-1,J)\}\right. \\
&\quad \left. + \{G_k(I,J) - G_k(I+1,J)\}\right|, \\
C_{kv}(I,J) &= \left|\{G_k(I,J) - G_k(I,J-1)\}\right. \\
&\quad \left. + \{G_k(I,J) - G_k(I,J+1)\}\right|, \\
2 \le I \le (M-1),\ 2 \le J &\le (N-1)
\end{aligned}
\tag{2}
$$

where $C_{kh}(I, J)$ is the local area contrast in the horizonal direction; and $C_{kv}(I, J)$ is the local area contrast in the vertical direction. In wood specimens, horizontal contrast $C_{kh}(I, J)$ was made up of not only a gloss change but also a brightness change in an annual ring, i.e., a change from earlywood (bright) to latewood (dark). To avoid calculating this type of brightness change, vertical contrasts $C_{kv}(I, J)$ were used as $C_k(I, J)$ in the next step.

Finally local area contrasts were summed up and averaged for every mosaic image.

$$
C_k = \frac{1}{(M-2)(N-2)} \sum_{I=2}^{M-1} \sum_{J=2}^{N-1} C_k(I,J) \tag{3}
$$

C_k was called "contrast" in this study. Relations between filter size k and contrast C_k were investigated, and the results are shown in the third line of Figs. 2 and 6 (see below).

Fractal analysis

In addition to the multiresolutional contrast analysis, fractal dimensions were calculated for each gloss image. In the general fractal image analysis, fractal dimension D is used as an index of the self-similarity of the image. We tried to use the fractal dimension D as an objective index of the characteristics of a gloss image from a micro to a macro scale.

The calculation procedure[11,12] was as follows: A 256-pixel square subset was set on a gloss image. A subset was divided in r-pixel squares (Fig. 5a), where r was 1–16 in this study. Gray levels at the corner of the r-pixel square were scaled in

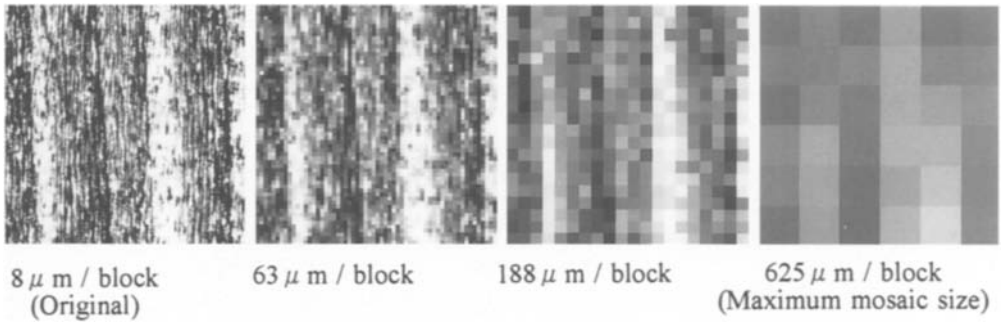

Fig. 4. Examples of mosaic images used in the multiresolutional contrast analysis. Specimen was a solid wood of Douglas fir illuminated perpendicular to the grain

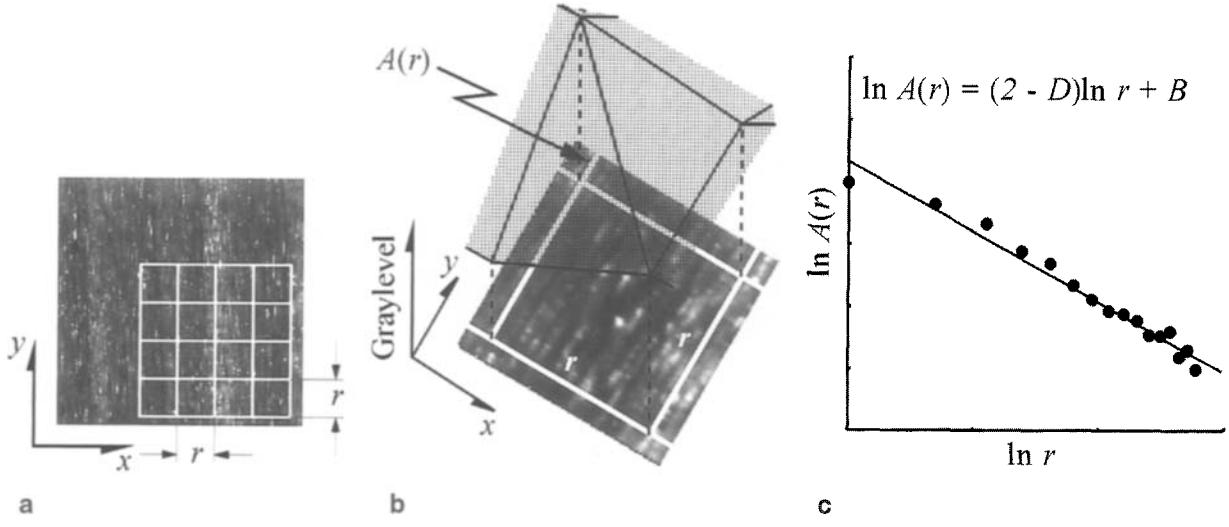

Fig. 5. Flow for calculation of fractal dimension D. **a** Coarse division by r-square mesh. **b** Calculation of image surface area. $A(r)$ is the total area of small triangles covering the image divided by r-square mesh. **c** Relations between $A(r)$ and r in the two-logarithmic coordinates. B, constant; D, fractal dimension

the z-direction. Many small triangles were formed continuously, and they covered the subset. Areas of all small triangles were accumulated, and it was defined as $A(r)$ (Fig. 5b). Relations between r and $A(r)$ were plotted on a double logarithmic chart (Fig. 5c). In most of the natural images, these plotted dots show the clear linear relation. This relation is expressed as Eq. 4.

$$\ln A(r) = (2 - D)\ln r + B \quad (4)$$

where D is a fractal dimension; and B is a constant. A slope of the linear regression line, which was an approximation of $(2 - D)$ in Eq. 4, was calculated, and the fractal dimension D was given. Altogether 10 subsets were set at different positions along the diagonal line with the same interval in a gloss image, and 10 D values were calculated. The average of 10 Ds was used as a fractal dimension of the gloss image. As the difference of gray levels between r-pixel square's corners becomes larger, an area of the triangle becomes larger as well (Fig. 5b). In other words, as changes in the brightness of a gloss image become larger and more frequently, the accumulated area $A(r)$ becomes larger too. As a result, D reflects characteristics of a gloss image and becomes a numerical index of the gloss.

Results and discussion

Multiresolutional contrast analysis

As shown in Fig. 3, gloss images illuminated parallel to the grain were darker and had fewer bright spots than gloss images illuminated perpendicular to the grain. Similar appearances were observed in most of the wood specimens including WPCs. Gloss images illuminated perpendicular to the grain only were used in these analyses because gloss images illuminated parallel to the grain were too dark and had fewer bright spots to analyze gloss.

All four photographs in the top line of Fig. 2 look like real oak wood, but their gloss images in the second line are fairly different from each other. For example, a gloss image of a mizunara (Japanese oak) has a lot of clear, small bright spots, but another three images have fewer or dull ones. In a gloss image of a printed grain, regularly arranged ink dots are visible. These visual differences among four gloss images are reflected in the contrast distributions of the third line of Fig. 2. Figure 6 shows the distributions of the rest of the 20 specimens.

As shown in Figs. 2 and 6, solid wood specimens have clear peaks at nearly 0.1 mm of the mosaic block size. In another specimen this peak becomes a dull shoulder or disappears. The levels of the contrast C_k of solid wood specimens are higher than those of other specimens in small to medium mosaic sizes (0.01–1.00 mm).

Figure 7 shows the relations between the maximum contrast and the smallest area contrast. The former corresponds to the most marked change of brightness in the middle mosaic size in an 8-mm square gloss image. The latter is the smallest mosaic size (8 μm square) of a 4-mm square gloss image. In Fig. 7 the solid wood specimens have relatively high values not only in the middle mosaic size but also in the smallest mosaic size; but even if wood was used as a base material, processed surfaces have lower contrast in the smallest mosaic size. Two granite specimens have the same levels of contrast as solid wood specimens in the middle mosaic size, but in the smallest mosaic size their contrast is fairly low.

These results indicate that the multiresolutional contrast analysis can numerize the two-dimensional distribution of gloss objectively and effectively. Furthermore, it is worthy of mention that the multiresolutional contrast analysis also can reveal the essential difference of gloss among materials. In the above results, for example, the gloss of solid wood specimens is identified by higher contrast values in the relatively small area compared to other specimens. Because wood is a cellular material whose anatomical structures appear in its surface, results of the multiresolutional contrast analysis suggest reflection on small or micro structures of wood, such as cell lumens. This type of analysis is difficult to perform by conventional goniophotometry using a spot measurement.

Incidentally, we believe that the multiresolutional contrast analysis proposed here is applicable to one of the pattern numerizations used for studying the mechanism of human vision,[13] but we need further studies about this problem.

Fractal analysis

The four graphs in the bottom line of Fig. 2 are the results of fractal analysis. The slope of the plotted points is important here because it defines the fractal dimension D. In the bottom line of Fig. 2 the slopes for solid wood and the WPC specimens are steeper than those for the other two specimens. In 4-mm and 8-mm square gloss images, this tendency is particularly clear. In other words, the former two specimens have greater changes in brightness in a small region, and the latter two specimens are relatively monotonous.

Table 2 shows fractal dimension Ds of all 24 specimens in five gloss image sizes. Figure 8 illustrates the data in Table 2, divided into four groups. As mentioned above, the fractal dimension D corresponds to the changes of brightness. Ds of solid wood specimens (Fig. 8a) are high for all gloss image sizes in comparison with other materials. Most of them are larger than 2.5. Particularly, in 4-mm square gloss images, Ds of solid wood specimens are higher than those for the other specimens except the WPC specimens. It seems reasonable to say that resins used in WPC specimens have high transparency and low absorption of light, which is why the Ds of WPC specimens are almost the same as that for solid wood specimens. In contrast, other processed-wood specimens have low D values in 4-mm square gloss images (Fig. 8b). In clear-varnished specimens, for example, small pigments contained in varnish may stick to the surface of wood and may interrupt reflcetion.

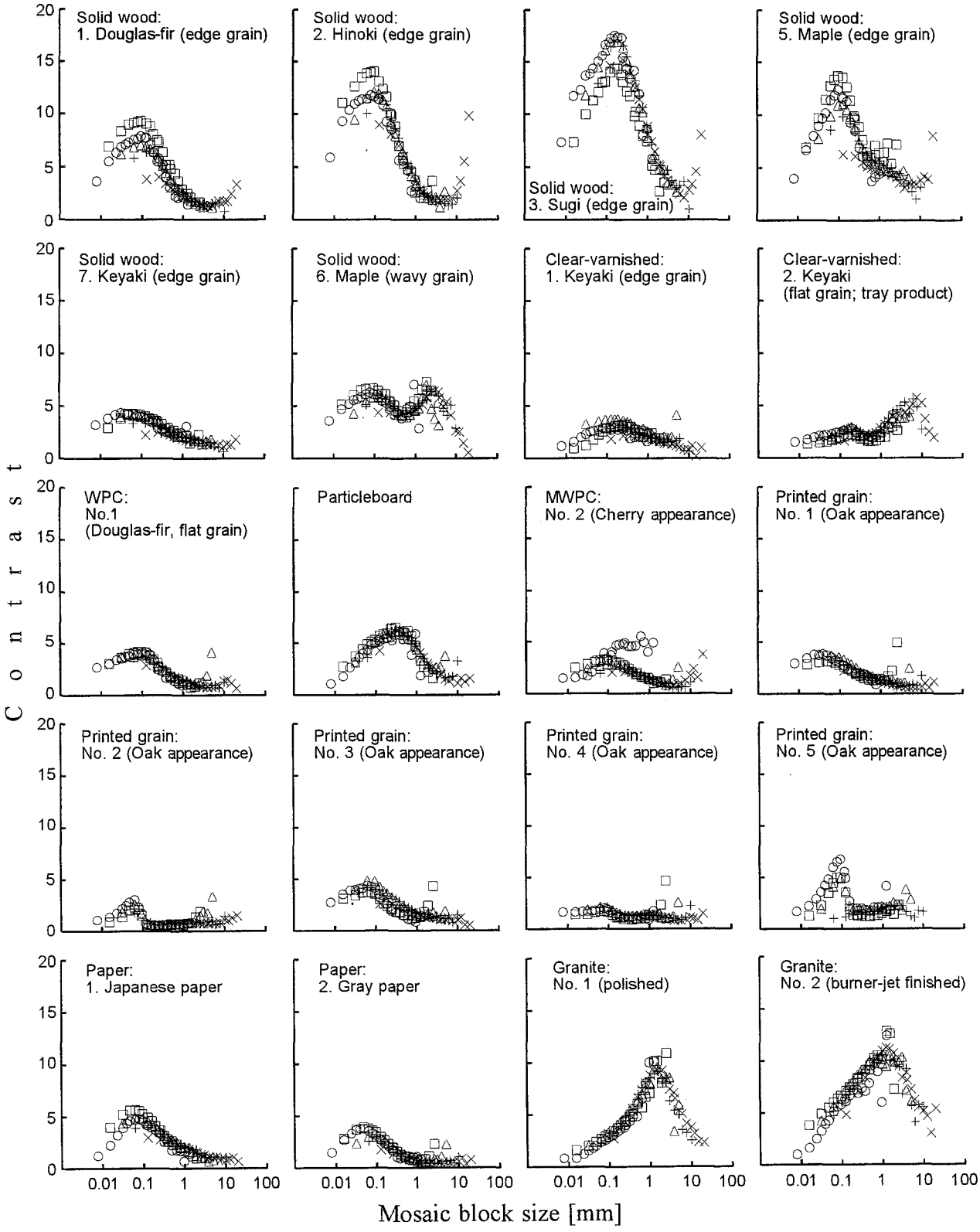

Fig. 6. Results of the multiresolutional contrast analysis. Illumination direction was perpendicular to the long side of the specimen. *Circles*, 4 mm square gloss image; *squares*, 8 mm square gloss image; *triangles*, 16 mm square gloss image; *pluses*, 32 mm square gloss image; *crosses*, 64 mm square gloss image

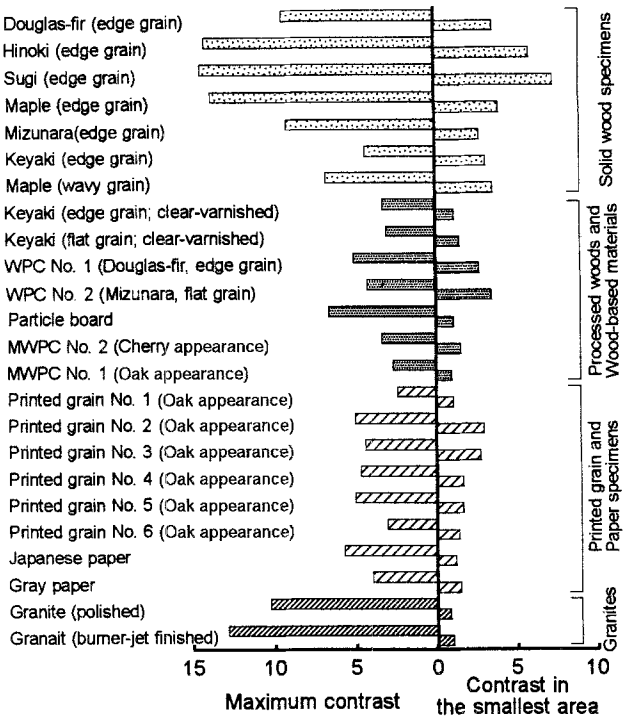

Fig. 7. Relations between the maximum contrast of a 8-mm square gloss image and contrast in the smallest area. Illumination direction was perpendicular to the grain or the long side of the specimen

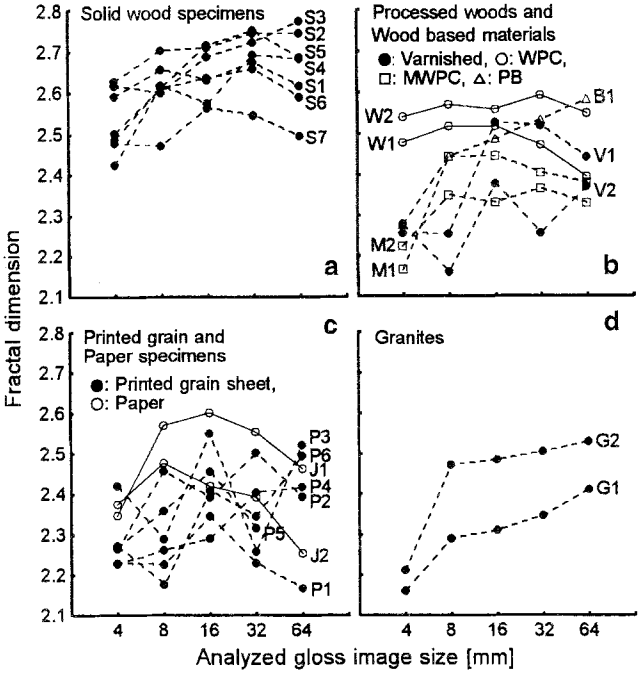

Fig. 8. Results of the fractal analyses. **a** seven solid wood specimens. **b** two clear varnished specimens, two wood–plastic composite (WPC) specimens, two milled wood–plastic composite (MWPC) specimens, and one particleboard (PB). **c** six printed grain sheets and two pieces of paper. **d** two granites. For the specimen numbers see Table 1

Table 2. Fractal dimensions

Specimen	Fractal dimensions				
	4 mm	8 mm	16 mm	32 mm	64 mm
Douglas fir (edge gain)	2.590	2.656	2.630	2.670	2.616
Hinoki (edge grain)	2.627	2.703	2.709	2.745	2.744
Sugi (edge grain)	2.616	2.600	2.687	2.723	2.774
Mizunara (edge grain)	2.424	2.617	2.574	2.692	2.681
Maple (edge grain)	2.486	2.612	2.715	2.751	2.685
Maple (wavy grain)	2.502	2.611	2.635	2.658	2.589
Keyaki (edge grain)	2.477	2.471	2.562	2.545	2.495
Keyaki (edge grain, clear-varnished)	2.255	2.253	2.526	2.518	2.442
Keyaki (flat grain, clear-varnished)	2.277	2.159	2.377	2.255	2.368
WPC No. 1 Douglas fir (edge grain)	2.477	2.517	2.517	2.471	2.393
WPC No. 2 Mizunara (flat grain)	2.539	2.568	2.557	2.590	2.547
Particle board	2.275	2.443	2.485	2.533	2.581
MWPC No. 1 (cherry appearance)	2.165	2.443	2.444	2.403	2.379
MWPC No. 2 (oak appearance)	2.223	2.348	2.331	2.364	2.329
Printed grain No. 1 (oak appearance)	2.229	2.226	2.344	2.229	2.167
Printed grain No. 2 (oak appearance)	2.264	2.457	2.392	2.502	2.393
Printed grain No. 3 (oak appearance)	2.420	2.289	2.551	2.258	2.522
Printed grain No. 4 (oak appearance)	2.227	2.261	2.291	2.405	2.416
Printed grain No. 5 (oak appearance)	2.269	2.358	2.455	2.316	–
Printed grain No. 6 (oak appearance)	2.272	2.176	2.408	2.345	2.494
Japanese paper	2.346	2.570	2.600	2.554	2.463
Gray paper	2.374	2.477	2.419	2.392	2.253
Granite (polished)	2.160	2.290	2.310	2.346	2.410
Granite (burner-jet finished)	2.211	2.470	2.484	2.505	2.530

From these results it is clear that the fractal analysis not only can numerize the two-dimensional distribution of gloss but also can indicate the essential difference of gloss among materials as well as the multiresolutional contrast analysis. One noteworthy point of the above results is that the gloss of solid wood specimens is characterized by wide and frequent changes of brightness in small areas. This finding is similar to the results of the multiresolutional contrast analysis.

Here, we must emphasize that it is new to use fractal dimensions as an index of brightness changes and not to use it for expressing self-similarity. We believe that the fractal dimension is a good index of brightness change, and fractal analysis is a useful image analyzing technique for comparing the gloss of wood with that of other materials, in addition to using multiresolutional contrast analysis.

Conclusions

Until now, it was difficult to measure and evaluate two-dimensionally the distributed gloss of a material. The two digital-image analyzing methods developed and used here – multiresolutional contrast analysis and fractal analysis – have made quantitative evaluation of gloss possible. The former method was based on calculating the multiresolutional contrast of the digital image. The latter method was based on calculation of fractal dimensions of images of various sizes. Both methods derived numerical indices for the frequency and magnitude of brightness variation in the image. The visual characteristics of gloss of materials were demonstrated quantitatively using these indices. It is our conclusion that both methods are useful tools for comparing the gloss of wood with that of other materials. Both methods can be applied to further investigations of the objective evaluation of gloss, and the influence of gloss on psychological visual images, for example.

Acknowledgment This study was supported in part by a Grant-in-Aid for Scientific Research (No. 07456079) from the Ministry of Education, Science, Sports, and Culture of Japan.

References

1. Kato H, Masuda M (1989) Anisotropic gloss of wood and light reflection at the surface of lumen (in Japanese). Bull Kyoto Univ For 61:292–300
2. Masuda M, Kato H, Horio Y (1989) Relation between properties of mechanically processed surfaces of wood and the gloss images (in Japanese) Bull Kyoto Univ For 61:301–309
3. Masuda M (1987) Visual characteristics of wood (in Japanese). In: Yamada T (ed) Mokushitsu kankyo no kagaku. Kaisei-Sha, Ohtsu, pp 105–114
4. Nagao M (1983) Pattern information processing (in Japanese). Corona-Sha, Tokyo, pp 29–40
5. Maekawa T, Fujita M, Saiki H (1993) Characterization of cell arrangement by polar coordinate analysis of power spectral patterns (in Japanese). J Soc Mater Sci Jpn 42:126–131
6. Fujita M, Kajita H, Maekawa T, Saiki H (1995) Evaluation of particle orientation by the Fourier transform image analysis (in Japanese). J Soc Mater Sci Jpn 44:267–272
7. Diao X, Furuno T, Uehara T (1996) Analysis of cell arrangements in softwood using two-dimensional fast Fourier transform. Mokuzai Gakkaishi 42:634–641
8. Diao X, Furuno T, Uehara T (1997) Analysis of vessel arrangements in hardwoods using two-dimensional fast Fourier transform. Mokuzai Gakkaishi 43:623–633
9. Nakamura M, Masuda M (1995) Visual characteristics of shadings in edge-grain patterns (in Japanese). Mokuzai Gakkaishi 41:301–308
10. Nakamura M, Masuda M, Imamichi K (1996) Description of visual characteristics of wood influencing some psychological images (in Japanese). Mokuzai Gakkaishi 42:1177–1187
11. Kaneko H (1987) Fractal feature and texture analysis (in Japanese). Trans Inst Electronics Information Commun Eng J70-D (5):964–972
12. Kamijo M, Nakazawa M, Shimizu Y, Kanai H (1996) Identification of nonwoven fabric by using sectional stochastic fractal variable (in Japanese). Seni Gakkaishi 52:112–121
13. Masuda M (1983) Studies on numerization of wood pattern and other patterns – especially on numerization of pattern based on flicker (in Japanese). J Soc Mater Sci Jpn 32:803–898